Journal of Applied Mathematics and Physics, 2017, 5, 2051-2071
http://www.scirp.org/journal/jamp
ISSN Online: 2327-4379
ISSN Print: 2327-4352

Computation of the Eigenvalues of 3*D* "Charged" Integral Equations

Diego Caratelli[1,2], Pierpaolo Natalini[3], Paolo E. Ricci[4]

[1]The Antenna Company, High Tech Campus, Eindhoven, the Netherlands
[2]Tomsk Polytechnic University, Tomsk, Russia
[3]Università degli Studi Roma Tre, Largo San Leonardo Murialdo, Roma, Italia
[4]International Telematic University UniNettuno, Corso Vittorio Emanuele II, Roma, Italia
Email: diego.caratelli@antennacompany.com, natalini@mat.uniroma3.it, paoloemilioricci@gmail.com

How to cite this paper: Caratelli, D., Natalini, P. and Ricci, P.E. (2017) Computation of the Eigenvalues of 3*D* "Charged" Integral Equations. *Journal of Applied Mathematics and Physics*, **5**, 2051-2071.
https://doi.org/10.4236/jamp.2017.510171

Received: October 7, 2017
Accepted: October 28, 2017
Published: October 31, 2017

Abstract

The Rayleigh-Ritz and the inverse iteration methods are used in order to compute the eigenvalues of 3*D* Fredholm-Stieltjes integral equations, *i.e.* 3*D* Fredholm equations with respect to suitable Stieltjes-type measures. Some applications are shown, relevant to the problem of computing the eigenvalues of a body charged by a finite number of masses concentrated on points, curves or surfaces lying in.

Keywords

3*D* Fredholm-Stieltjes Integral Equations, Eigenvalues, Rayleigh-Ritz Method, Inverse Iteration Method

1. Introduction

The theory of Fredholm integral equations is strictly connected with the birth of functional analysis. A background of this theory can be found in classical books (see e.g. [1] [2]). For recent developments relevant to numerical computation of solutions, see [3].

In [4] [5], the Author shows that the Fredholm theory still holds considering the so called charged Fredholm integral equations, *i.e.* Fredholm equations with respect to a Stieltjes measure obtained by adding to the ordinary Lebesgue measure a finite combination of positive masses concentrated in arbitrary points of the considered interval. A topic which at present is included, as a particular case, in the theory of strictly positive compact operators.

In the one-dimensional case, the mechanical interpretation of these equations is connected with the problem of the free vibrations of a string charged by a finite number of cursors, and is related to an extension of the classical orthogonality property of eigensolutions, called the "Sobolev-type" orthogonality (see e.g. [6] [7]).

In preceding articles [8] [9] [10], the problem of numerical computation of the above mentioned eigenvalue problems was solved, by using the so called inverse iteration method, showing applications in one and two-dimensional cases.

In this article, after briefly recalling the main results about the theory of eigenvalues for charged Fredholm integral equations, we mention how to obtain (in the particular case of a symmetric and strictly positive operator), the lower and upper approximations of these eigenvalues by means of the Rayleigh-Ritz method [1], [11] and the Fichera orthogonal invariants method [11] [12] respectively. Then we conclude by showing that, even in the three-dimensional case, the lower approximations of the eigenvalues obtained by means of the Rayleigh-Ritz method can be improved by applying the inverse iteration method [13]. Numerical computations relevant to the considered case are developed in the concluding section.

2. Lebesgue-Stieltjes Measures in a 3*D* Interval

Consider the interval $\mathcal{A}$ and the Hilbert space $L^2_{dM} \equiv L^2_{dM}(\mathcal{A})$ equipped with the scalar product

$$[U,V]_{dM} := (U,V)_{\rho(P)dP} + (U,V)_{\Delta_r} + (U,V)_{\Delta\gamma_n} + (U,V)_{\Delta_{\Sigma_m}} \tag{1}$$

where $[U,V]_{dM} \equiv (U,V)_{L^2_{dM}}$ and the subscripts "$\rho(P)\mathrm{d}P$", "Δ_r", "$\Delta\gamma_n$", "Δ_{Σ_m}" refer to the following definitions:

$$(U,V)_{\rho(P)dP} := \int_{\mathcal{A}} U(P)V(P)\rho(P)\,\mathrm{d}P \tag{2}$$

$$(U,V)_{\Delta_r} := \sum_{h=1}^{r} m_h U(A_h)V(A_h) \tag{3}$$

$$(U,V)_{\Delta\gamma_n} := \sum_{k=1}^{n} \int_{\gamma_k} \sigma_k\left(P(s)\right)U\left(P(s)\right)V\left(P(s)\right)\mathrm{d}s \tag{4}$$

and

$$(U,V)_{\Delta_{\Sigma_m}} := \sum_{\ell=1}^{m} \int_{\Sigma_\ell} \tau_\ell\left(P(u,v)\right)U\left(P(u,v)\right)V\left(P(u,v)\right)\mathrm{d}\sigma\,, \tag{5}$$

(obviously $\mathrm{d}\sigma := \sqrt{EG-F^2}\,\mathrm{d}u\mathrm{d}v$), so that the Stieltjes measure is the sum of the ordinary Lebesgue measure plus a finite sum of charges m_h concentrated on points $A_h \subset \bar{\mathcal{A}}$, $(h=1,2,\cdots,r)$, plus a finite sum of continuous charges belonging to the curves $\Sigma_\ell \subset \bar{\mathcal{A}}$, with densities $\sigma_k(\cdot)$, $(k=1,2,\cdots,n)$, plus a finite sum of continuous charges belonging to the surfaces $\Sigma_\ell \subset \bar{\mathcal{A}}$, with densities $\tau_k(\cdot)$, $(\ell=1,2,\cdots,m)$.

It is worth noting that $L^2_{dM}(\mathcal{A})$ is constituted by functions of the ordinary space $L^2(\mathcal{A})$, a (complete) Hilbert space, which does not have singularities (*i.e.* discontinuities) at points A_h, $(h=1,2,\cdots,r)$, at curves γ_k, $(k=1,2,\cdots,n)$, and surfaces Σ_ℓ, $(\ell=1,2,\cdots,m)$, according to the usual condition for existence of the relevant Stieltjes integrals (see e.g. [14]).

Let us consider, for example, the computation of integrals with respect to the above Dirac-type measures:

$$\int_{\mathcal{A}} K(P,Q)\varphi(Q)m_h\delta(A_h) = m_h K(P,A_h)\varphi(A_h)$$

$$\begin{aligned}&\int_{\mathcal{A}} K(P,Q)\varphi(Q)\int_{\gamma_k}\sigma_k(Q(s))\delta(Q(s))\mathrm{d}s\\&=\int_{\gamma_k}K(P,Q(s))\varphi(Q(s))\tau_\ell(Q(s))\mathrm{d}s\end{aligned}$$

$$\begin{aligned}&\int_{\mathcal{A}} K(P,Q)\varphi(Q)\int_{\Sigma_\ell}\tau_\ell(Q(u,v))\delta(Q(u,v))\mathrm{d}\sigma\\&=\int_{\Sigma_\ell}K(P,Q(u,v))\varphi(Q(u,v))\tau_\ell(Q(u,v))\mathrm{d}\sigma\end{aligned}$$

These formulas will be useful in the following.

The Eigenvalue Problem for 3D "Charged" Operators

Consider in $L^2_{dM}(\mathcal{A})$ the eigenvalue problem

$$\mathcal{K}\varphi = \mu\varphi \tag{6}$$

$$\mathcal{K}\varphi(\cdot) := \int_{\mathcal{A}} K(\cdot,Q)\varphi(Q)\mathrm{d}M_Q \tag{7}$$

where $K(P,Q)$ is a symmetric kernel, and

$$\begin{aligned}\mathrm{d}M_Q &= \rho(Q)\mathrm{d}Q + \sum_{h=1}^{r} m_h\delta(A_h) + \sum_{k=1}^{n}\int_{\gamma_k}\sigma_k(Q(s))\delta(Q(s))\mathrm{d}s\\&\quad+\sum_{\ell=1}^{m}\int_{\Sigma_\ell}\tau_\ell(Q(u,v))\delta(Q(u,v))\mathrm{d}\sigma\end{aligned} \tag{8}$$

(δ denoting the usual Dirac-Delta function).

According to the above positions, we have

$$\begin{aligned}(\mathcal{K}\varphi)(P) &= \int_{\mathcal{A}} K(P,Q)\varphi(Q)\rho(Q)\mathrm{d}Q + \sum_{h=1}^{r} m_h K(P,A_h)\varphi(A_h)\\&\quad+\sum_{k=1}^{n}\int_{\mathcal{A}}\int_{\gamma_k}K(P,Q)\varphi(Q(s))\sigma_k(Q(s))\delta(Q(s))\mathrm{d}s\\&\quad+\sum_{\ell=1}^{m}\int_{\mathcal{A}}\int_{\Sigma_\ell}K(P,Q)\varphi(Q(s))\tau_\ell(Q(u,v))\delta(Q(u,v))\mathrm{d}\sigma\\&=(K(P,Q),\varphi(Q))_{\rho(Q)dQ} + (K(P,Q),\varphi(Q))_{\Delta_r(Q)}\\&\quad+(K(P,Q),\varphi(Q))_{\Delta\gamma_n(Q)} + (K(P,Q),\varphi(Q))_{\Delta_{\Sigma_m}(Q)}\end{aligned} \tag{9}$$

so that

$$\begin{aligned}[\mathcal{K}U,V]_{dM} &= ((\mathcal{K}U)(P),V(P))_{\rho(P)dP} + ((\mathcal{K}U)(P),V(P))_{\Delta_r(P)}\\&\quad+((\mathcal{K}U)(P),V(P))_{\Delta_{\gamma_n}(P)}\end{aligned}$$

i.e., by using scalar products, with respect to the relevant measures:

$$
\begin{aligned}
&[\mathcal{K}U,V]_{dM}\\
&=\Big(\big(K(P,Q),U(Q)\big)_{\rho(Q)dQ},V(P)\Big)_{\rho(P)dP}+\Big(\big(K(P,Q),U(Q)\big)_{\Delta_r(Q)},V(P)\Big)_{\rho(P)dP}\\
&\quad+\Big(\big(K(P,Q),U(Q)\big)_{\Delta\gamma_n(Q)},V(P)\Big)_{\rho(P)dP}+\Big(\big(K(P,Q),U(Q)\big)_{\Delta_{\Sigma_m}(Q)},V(P)\Big)_{\rho(P)dP}\\
&\quad+\Big(\big(K(P,Q),U(Q)\big)_{\rho(Q)dQ},V(P)\Big)_{\Delta_r(P)}+\Big(\big(K(P,Q),U(Q)\big)_{\Delta_r(Q)},V(P)\Big)_{\Delta_r(P)}\\
&\quad+\Big(\big(K(P,Q),U(Q)\big)_{\Delta\gamma_n(Q)},V(P)\Big)_{\Delta_r(P)}+\Big(\big(K(P,Q),U(Q)\big)_{\Delta_{\Sigma_m}(Q)},V(P)\Big)_{\Delta_r(P)}\\
&\quad+\Big(\big(K(P,Q),U(Q)\big)_{\rho(Q)dQ},V(P)\Big)_{\Delta\gamma_n(P)}+\Big(\big(K(P,Q),U(Q)\big)_{\Delta_r(Q)},V(P)\Big)_{\Delta\gamma_n(P)}\\
&\quad+\Big(\big(K(P,Q),U(Q)\big)_{\Delta\gamma_n(Q)},V(P)\Big)_{\Delta\gamma_n(P)}+\Big(\big(K(P,Q),U(Q)\big)_{\Delta_{\Sigma_m}(Q)},V(P)\Big)_{\Delta\gamma_n(P)}\\
&\quad+\Big(\big(K(P,Q),U(Q)\big)_{\rho(Q)dQ},V(P)\Big)_{\Delta_{\Sigma_m}(P)}+\Big(\big(K(P,Q),U(Q)\big)_{\Delta_r(Q)},V(P)\Big)_{\Delta_{\Sigma_m}(P)}\\
&\quad+\Big(\big(K(P,Q),U(Q)\big)_{\Delta\gamma_n(Q)},V(P)\Big)_{\Delta_{\Sigma_m}(P)}+\Big(\big(K(P,Q),U(Q)\big)_{\Delta_{\Sigma_m}(Q)},V(P)\Big)_{\Delta_{\Sigma_m}(P)}
\end{aligned}
$$

Furthermore

$$
\begin{aligned}
&\Big(\big(K(P,Q),U(Q)\big)_{\rho(Q)dQ},V(P)\Big)_{\rho(P)dP}\\
&=\iint_{\mathcal{A}\times\mathcal{A}}K(P,Q)U(Q)V(P)\rho(P)\rho(Q)\,\mathrm{d}P\mathrm{d}Q
\end{aligned}
$$

$$
\begin{aligned}
&\Big(\big(K(P,Q),U(Q)\big)_{\Delta_r(Q)},V(P)\Big)_{\rho(P)dP}\\
&=\sum_{h=1}^{r}m_hU(A_h)\int_{\mathcal{A}}K(P,A_h)V(P)\rho(P)\,\mathrm{d}P
\end{aligned}
$$

$$
\begin{aligned}
&\Big(\big(K(P,Q),U(Q)\big)_{\rho(Q)dQ},V(P)\Big)_{\Delta_r(P)}\\
&=\sum_{h=1}^{r}m_hV(A_h)\int_{\mathcal{A}}K(P,A_h)U(P)\rho(P)\,\mathrm{d}P
\end{aligned}
$$

where we used the symmetry of the kernel,

$$
\begin{aligned}
&\Big(\big(K(P,Q),U(Q)\big)_{\Delta\gamma_n(Q)},V(P)\Big)_{\rho(P)dP}\\
&=\sum_{k=1}^{n}\int_{\gamma_k}\int_{\mathcal{A}}K\big(P,Q(s)\big)U\big(Q(s)\big)\tau_\ell\big(Q(s)\big)V(P)\rho(P)\,\mathrm{d}s\mathrm{d}P
\end{aligned}
$$

$$
\begin{aligned}
&\Big(\big(K(P,Q),U(Q)\big)_{\rho(Q)dQ},V(P)\Big)_{\Delta\gamma_n(P)}\\
&=\sum_{k=1}^{n}\int_{\gamma_k}\int_{\mathcal{A}}K\big(P,Q(s)\big)V\big(Q(s)\big)\sigma_k\big(Q(s)\big)U(P)\rho(P)\,\mathrm{d}s\mathrm{d}P
\end{aligned}
$$

$$
\begin{aligned}
\Big(\big(K(P,Q),U(Q)\big)_{\Delta_{\Sigma_m}(Q)},V(P)\Big)_{\Delta_{\Sigma_m}(P)}&=\sum_{j=1}^{m}\sum_{\ell=1}^{m}\int_{\Sigma_j}\int_{\Sigma_\ell}K\big(P(t,w),Q(u,v)\big)U\big(Q(u,v)\big)\\
&\quad\times V\big(P(t,w)\big)\tau_\ell\big(Q(u,v)\big)\tau_\ell\big(P(t,w)\big)\,\mathrm{d}\sigma_1\mathrm{d}\sigma_2
\end{aligned}
$$

where we used the symmetry of the kernel,

$$\left(\left(K(P,Q),U(Q)\right)_{\Delta_{\Sigma_m}(Q)},V(P)\right)_{\rho(P)dP}$$
$$=\sum_{\ell=1}^{m}\int_{\Sigma_\ell}\int_{\mathcal{A}}K\left(P,Q(u,v)\right)U\left(Q(u,v)\right)\tau_\ell\left(Q(u,v)\right)V(P)\rho(P)\,\mathrm{d}\sigma\,\mathrm{d}P$$
$$\left(\left(K(P,Q),U(Q)\right)_{\rho(Q)dQ},V(P)\right)_{\Delta_{\Sigma_m}(P)}$$
$$=\sum_{\ell=1}^{m}\int_{\Sigma_\ell}\int_{\mathcal{A}}K\left(P,Q(u,v)\right)V\left(Q(u,v)\right)\tau_\ell\left(Q(u,v)\right)U(P)\rho(P)\,\mathrm{d}\sigma\,\mathrm{d}P$$

where we used the symmetry of the kernel,

$$\left(\left(K(P,Q),U(Q)\right)_{\Delta_r(Q)},V(P)\right)_{\Delta_r(P)}$$
$$=\sum_{h=1}^{r}\sum_{j=1}^{r}m_h m_j K\left(A_h,A_j\right)U\left(A_h\right)V\left(A_j\right)$$

$$\left(\left(K(P,Q),U(Q)\right)_{\Delta_{\gamma_n}(Q)},V(P)\right)_{\Delta_r(P)}$$
$$=\sum_{h=1}^{r}m_h V\left(A_h\right)\sum_{k=1}^{n}\int_{\gamma_k}K\left(A_h,Q(s)\right)U\left(Q(s)\right)\sigma_k\left(Q(s)\right)\mathrm{d}s$$
$$\left(\left(K(P,Q),U(Q)\right)_{\Delta_r(Q)},V(P)\right)_{\Delta_{\gamma_n}(P)}$$
$$=\sum_{h=1}^{r}m_h U\left(A_h\right)\sum_{k=1}^{n}\int_{\gamma_k}K\left(A_h,Q(s)\right)V\left(Q(s)\right)\sigma_k\left(Q(s)\right)\mathrm{d}s$$

where we used the symmetry of the kernel,

$$\left(\left(K(P,Q),U(Q)\right)_{\Delta_{\Sigma_m}(Q)},V(P)\right)_{\Delta_r(P)}$$
$$=\sum_{h=1}^{r}m_h V\left(A_h\right)\sum_{\ell=1}^{m}\int_{\Sigma_\ell}K\left(A_h,Q(u,v)\right)U\left(Q(u,v)\right)\tau_\ell\left(Q(u,v)\right)\mathrm{d}\sigma$$
$$\left(\left(K(P,Q),U(Q)\right)_{\Delta_r(Q)},V(P)\right)_{\Delta_{\Sigma_m}(P)}$$
$$=\sum_{h=1}^{r}m_h U\left(A_h\right)\sum_{\ell=1}^{m}\int_{\Sigma_\ell}K\left(A_h,Q(u,v)\right)V\left(Q(u,v)\right)\tau_\ell\left(Q(u,v)\right)\mathrm{d}\sigma$$

where we used the symmetry of the kernel,

$$\left(\left(K(P,Q),U(Q)\right)_{\Delta_{\Sigma_m}(Q)},V(P)\right)_{\Delta_{\gamma_n}(P)}$$
$$=\sum_{k=1}^{n}V\left(P(s)\right)\sigma_k\left(P(s)\right)\sum_{\ell=1}^{m}\int_{\Sigma_\ell}K\left(P(s),Q(u,v)\right)U\left(Q(u,v)\right)\tau_\ell\left(Q(u,v)\right)\mathrm{d}\sigma\,\mathrm{d}s$$
$$\left(\left(K(P,Q),U(Q)\right)_{\Delta_{\gamma_n}(Q)},V(P)\right)_{\Delta_{\Sigma_m}(P)}$$
$$=\sum_{k=1}^{n}U\left(P(s)\right)\sigma_k\left(P(s)\right)\sum_{\ell=1}^{m}\int_{\Sigma_\ell}K\left(P(s),Q(u,v)\right)V\left(Q(u,v)\right)\tau_\ell\left(Q(u,v)\right)\mathrm{d}\sigma\,\mathrm{d}s$$

where we used the symmetry of the kernel, and lastly

$$\left(\left(K(P,Q),U(Q)\right)_{\Delta\gamma_n(Q)},V(P)\right)_{\Delta\gamma_n(P)}$$
$$=\sum_{k=1}^{n}\sum_{\ell=1}^{n}\int_{\gamma_k}\int_{\gamma_\ell}K\left(P(\sigma),Q(s)\right)U\left(Q(s)\right)V\left(P(\sigma)\right)\sigma_k\left(Q(s)\right)\sigma_\ell\left(P(\sigma)\right)\mathrm{d}s\mathrm{d}\sigma$$

$$\left(\left(K(P,Q),U(Q)\right)_{\Delta_{\Sigma_m}(Q)},V(P)\right)_{\Delta_{\Sigma_m}(P)}$$
$$=\sum_{j=1}^{m}\sum_{\ell=1}^{m}\int_{\Sigma_j}\int_{\Sigma_\ell}K\left(P(t,w),Q(u,v)\right)U\left(Q(u,v)\right)$$
$$\times V\left(P(t,w)\right)\tau_\ell\left(Q(u,v)\right)\tau_\ell\left(P(t,w)\right)\mathrm{d}\sigma_1\mathrm{d}\sigma_2$$

3. Computation of the Eigenvalues for Charged Integral Equations

The computation of the eigenvalues of second kind Fredholm integral equations is usually performed by using the Rayleig-Ritz method [1] [11] for lower bounds, and the Fichera orthogonal invariants method [11] [12] for upper bounds. An alternative procedure, called the *inverse iteration method*, can be used to improve the lower approximations previously obtained by means of the Rayleigh-Ritz method. This approach was already considered in [13], and will be applied even in the present case.

We will not describe herewith the three above mentioned methods, because they are essentially independent of the dimension of the considered vibrating item (string, membrane or body). We refer for shortness to the above mentioned articles [8] [9] [11] [12].

4. Applications

Let $\mathcal{A}\equiv[0,a]\times[0,b]\times[0,c]$, $O\equiv(0,0,0),U\equiv(a,b,c)$,

$$P\equiv(x_P,y_P,z_P),\ Q\equiv(x_Q,y_Q,z_Q),\ R\equiv(x_P,y_P,z_Q),\ S\equiv(x_P,y_Q,z_Q)$$
$$T\equiv(x_Q,y_P,z_P),\ L\equiv(x_Q,y_Q,z_P),\ M\equiv(x_P,y_Q,z_P),\ N\equiv(x_Q,y_P,z_Q)$$
$$0\le x_P\le a,\ 0\le y_P\le b,\ 0\le z_P\le c$$
$$0\le x_Q\le a,\ 0\le y_Q\le b,\ 0\le z_Q\le c$$

$$K(P,Q)=\begin{cases}\overline{OP}\cdot\overline{UQ}, & \text{if } x_P\le x_Q, y_P\le y_Q, z_P\le z_Q,\\ \overline{OQ}\cdot\overline{UP}, & \text{if } x_P\ge x_Q, y_P\ge y_Q, z_P\ge z_Q,\\ \overline{OR}\cdot\overline{UL}, & \text{if } x_P\le x_Q, y_P\le y_Q, z_P\ge z_Q,\\ \overline{OS}\cdot\overline{UT}, & \text{if } x_P\le x_Q, y_P\ge y_Q, z_P\ge z_Q,\\ \overline{OT}\cdot\overline{US}, & \text{if } x_P\ge x_Q, y_P\le y_Q, z_P\le z_Q,\\ \overline{OL}\cdot\overline{UR}, & \text{if } x_P\ge x_Q, y_P\ge y_Q, z_P\le z_Q,\\ \overline{OM}\cdot\overline{UN}, & \text{if } x_P\le x_Q, y_P\ge y_Q, z_P\le z_Q,\\ \overline{ON}\cdot\overline{UM}, & \text{if } x_P\ge x_Q, y_P\le y_Q, z_P\ge z_Q,\end{cases} \tag{1}$$

i.e.

$$K(P,Q)=\begin{cases}\sqrt{x_P^2+y_P^2+z_P^2}\sqrt{(a-x_Q)^2+(b-y_Q)^2+(c-z_Q)^2}, & \text{if } x_P\le x_Q, y_P\le y_Q, z_P\le z_Q,\\ \sqrt{x_Q^2+y_Q^2+z_Q^2}\sqrt{(a-x_P)^2+(b-y_P)^2+(c-z_P)^2}, & \text{if } x_P\ge x_Q, y_P\ge y_Q, z_P\ge z_Q,\\ \sqrt{x_P^2+y_P^2+z_Q^2}\sqrt{(a-x_Q)^2+(b-y_Q)^2+(c-z_P)^2}, & \text{if } x_P\le x_Q, y_P\le y_Q, z_P\ge z_Q,\\ \sqrt{x_P^2+y_Q^2+z_Q^2}\sqrt{(a-x_Q)^2+(b-y_P)^2+(c-z_P)^2}, & \text{if } x_P\le x_Q, y_P\ge y_Q, z_P\ge z_Q,\\ \sqrt{x_Q^2+y_P^2+z_P^2}\sqrt{(a-x_P)^2+(b-y_Q)^2+(c-z_Q)^2}, & \text{if } x_P\ge x_Q, y_P\le y_Q, z_P\le z_Q,\\ \sqrt{x_Q^2+y_Q^2+z_P^2}\sqrt{(a-x_P)^2+(b-y_P)^2+(c-z_Q)^2}, & \text{if } x_P\ge x_Q, y_P\ge y_Q, z_P\le z_Q,\\ \sqrt{x_P^2+y_Q^2+z_P^2}\sqrt{(a-x_Q)^2+(b-y_P)^2+(c-z_Q)^2}, & \text{if } x_P\le x_Q, y_P\ge y_Q, z_P\le z_Q,\\ \sqrt{x_Q^2+y_P^2+z_Q^2}\sqrt{(a-x_P)^2+(b-y_Q)^2+(c-z_P)^2}, & \text{if } x_P\ge x_Q, y_P\le y_Q, z_P\ge z_Q.\end{cases}$$

Obviously $K(P,Q)=K(Q,P)$, *i.e.* the kernel is symmetric, and even positive definite, since $K(P,Q)>0$, $\forall(P,Q)\in\mathcal{A}$.

Consider in $L^2_{dM}(\mathcal{A})$ the eigenvalue problem

$$\mathcal{K}\varphi=\mu\varphi \tag{2}$$

$$\mathcal{K}\varphi:=\int_{\mathcal{A}}K(\cdot,Q)\varphi(Q)\mathrm{d}M_Q \tag{3}$$

where

$$\mathrm{d}M_Q=\rho(Q)\mathrm{d}Q+\sum_{h=1}^{r}m_h\delta(A_h)+\sum_{k=1}^{n}\int_{\gamma_k}\sigma_k(Q(s))\delta(Q(s))\mathrm{d}s$$
$$+\sum_{\ell=1}^{m}\int_{\Sigma_\ell}\tau_\ell(Q(u,v))\delta(Q(u,v))\mathrm{d}\sigma$$

(δ denoting the usual Dirac-Delta function).

The considered operator is compact and strictly positive, since it is connected with free vibrations of a body charged by a finite number of masses concentrated on points, curves, or surfaces contained in $\mathcal{A}$.

Numerical Example 1

Let $a=b=c=1$, and $\mathrm{d}M=\rho(x,y,z)\mathrm{d}x\mathrm{d}y\mathrm{d}z$ with $\rho(x,y,z)=1+2x+3y+4z$ (see **Figure 1**). Under this assumption, the apprpximate eigenvalues evaluated by using the Rayleigh-Ritz and inverse iteration methods are listed in **Table 1**, whereas the relevant eigenfunctions are shown in **Figure 2**.

Numerical Example 2

Let $a=b=c=1$, and $\mathrm{d}M=\rho(x,y,z)\mathrm{d}x\mathrm{d}y\mathrm{d}z$ with $\rho(x,y,z)=8\pi^3\mathrm{e}^{-(x+y+z)^2}\sin(\pi xyz)$ (see **Figure 3**). Under this assumption, the approximate eigenvalues evaluated by using the Rayleigh-Ritz and inverse iteration methods are listed in **Table 2**, whereas the relevant eigenfunctions are shown in **Figure 4**.

Numerical Example 3

Let $a=b=c=1$, and

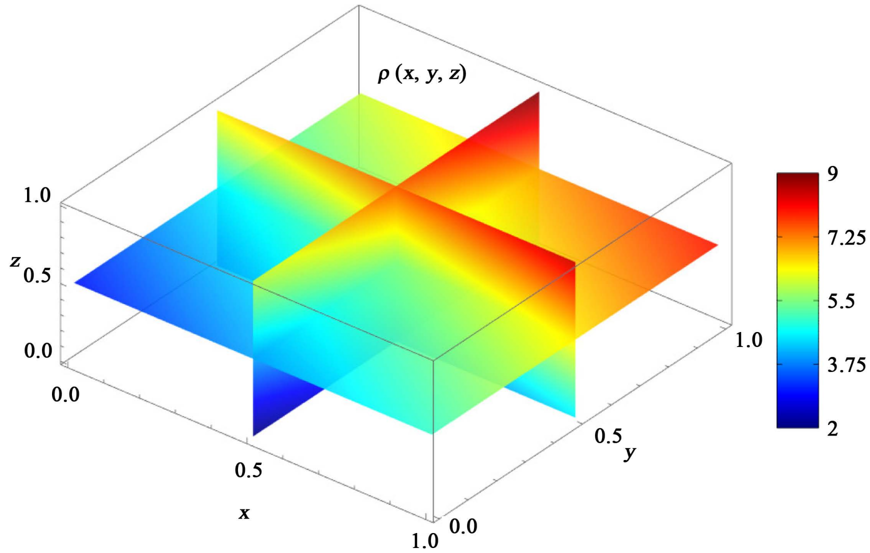

Figure 1. Spatial distribution of the volume density function $\rho(x, y, z)$ relevant to the numerical Example 1.

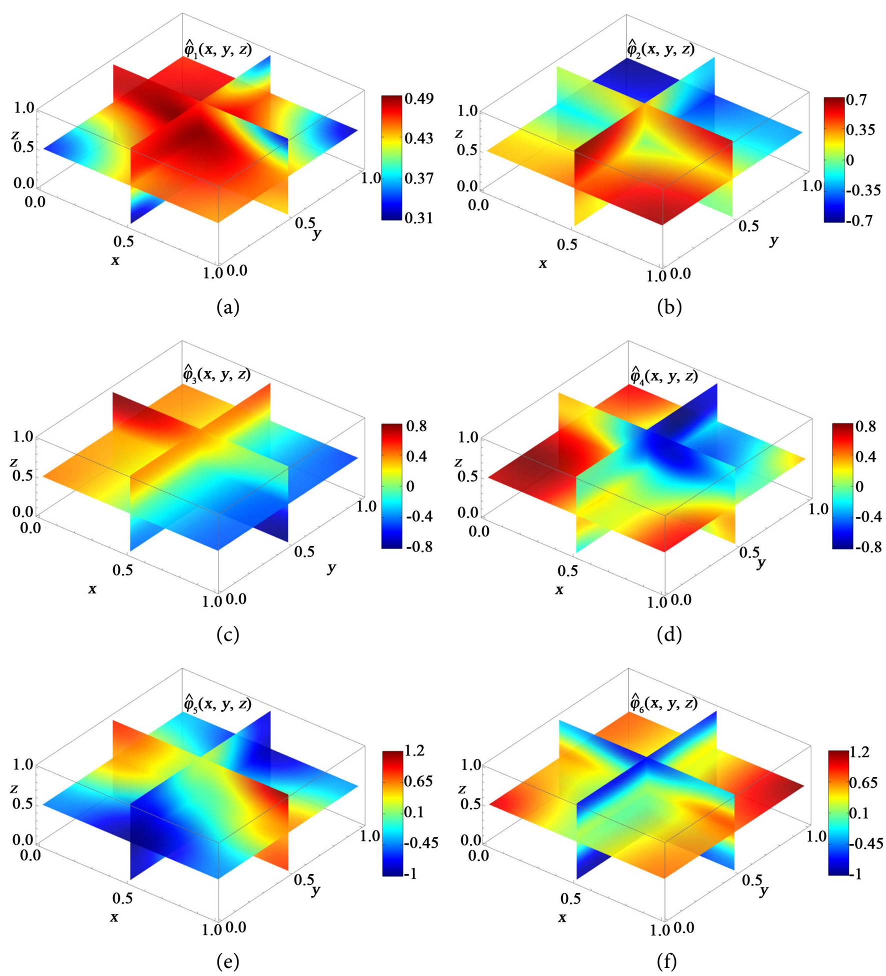

Figure 2. Spatial distribution of the approximate eigenfunctions $\hat{\varphi}_h(x, y, z)$ $(h = 1, 2, \cdots, 6)$ relevant to the numerical Example 1.

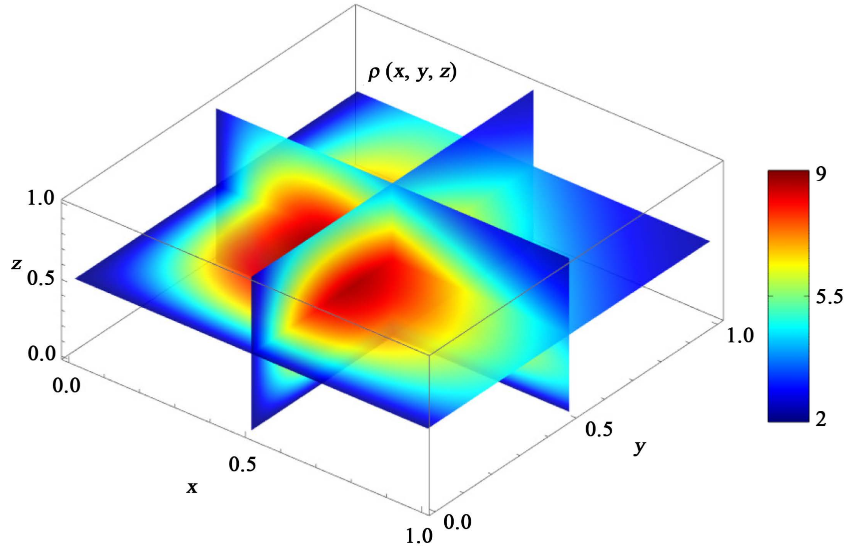

Figure 3. Spatial distribution of the volume density function $\rho(x, y, z)$ relevant to the numerical Example 2.

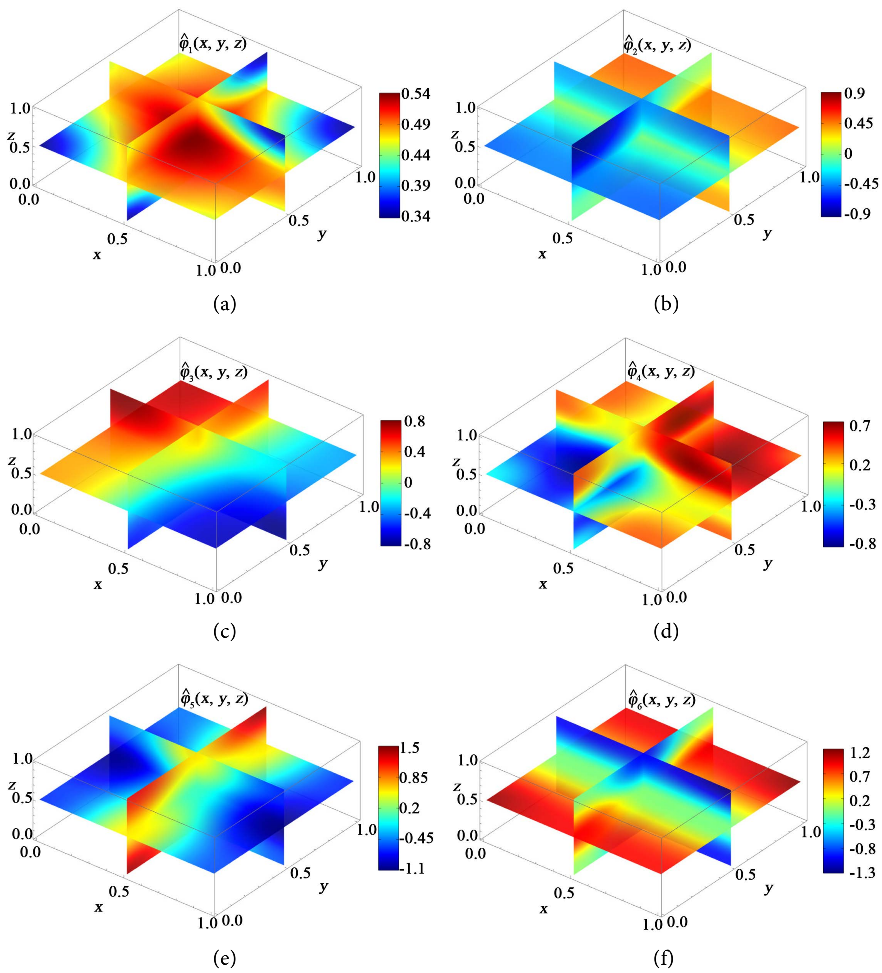

Figure 4. Spatial distribution of the approximate eigenfunctions $\hat{\varphi}_h(x, y, z)$ ($h = 1, 2, \cdots, 6$) relevant to the numerical Example 2.

Table 1. Approximate eigenvalues $\tilde{\mu}_h$ and $\hat{\mu}_h$ ($h = 1, 2, \cdots, 6$) relevant to the numerical Example 1, as computed by means of the Rayleigh-Ritz and inverse iteration method, respectively.

h	$\tilde{\mu}_h$	$\hat{\mu}_h$
1	2.30919	2.30934
2	0.584150	0.584855
3	0.580232	0.580932
4	0.144731	0.145178
5	0.136953	0.137599
6	0.135077	0.135689

Table 2. Approximate eigenvalues $\tilde{\mu}_h$ and $\hat{\mu}_h$ ($h = 1, 2, \cdots, 6$) relevant to the numerical Example 2, as computed by means of the Rayleigh-Ritz and inverse iteration method, respectively.

h	$\tilde{\mu}_h$	$\hat{\mu}_h$
1	1.97474	1.97528
2	0.396395	0.396914
3	0.396395	0.396914
4	0.0957090	0.0960668
5	0.0912646	0.0917548
6	0.0912646	0.0917548

$$\mathrm{d}M = \rho(x, y, z)\,\mathrm{d}x\mathrm{d}y\mathrm{d}z + \delta\left(x - \frac{1}{2}\right)\delta\left(y - \frac{1}{2}\right)\delta\left(z - \frac{1}{2}\right)\mathrm{d}x\mathrm{d}y\mathrm{d}z$$

with $\rho(x, y, z) = \mathrm{e}^{-x-y-z}$ (see Figure 5). Under this assumption, the approximate eigenvalues evaluated by using the Rayleigh-Ritz and inverse iteration methods are listed in Table 3, whereas the relevant eigenfunctions are shown in Figure 6.

Numerical Example 4

Let $a = b = c = 1$, and
$\mathrm{d}M = \rho(x, y, z)\,\mathrm{d}x\mathrm{d}y\mathrm{d}z + \sum_h m_h \delta(x - x_h)\delta(y - y_h)\delta(z - z_h)\,\mathrm{d}x\mathrm{d}y\mathrm{d}z$ with $\rho(x, y, z) = 2\log\left(1 + z\left(1 + y(1 + x)\right)\right)$, and $m_h = 1/(x_h + y_h + z_h)$, $x_h = y_h = z_h = \dfrac{1}{H}\left(h - \dfrac{1}{2}\right)$ for $h = 1, 2, 3 = H$ (see Figure 7). Under this assumption, the approximate eigenvalues evaluated by using the Rayleigh-Ritz and inverse iteration methods are listed in Table 4, whereas the relevant eigenfunctions are shown in Figure 8.

Numerical Example 5

Let $a = b = c = 1$, and
$\mathrm{d}M = \rho(x, y, z)\,\mathrm{d}x\mathrm{d}y\mathrm{d}z + \sum_h m_h \delta(x - x_h)\delta(y - y_h)\delta(z - z_h)\,\mathrm{d}x\mathrm{d}y\mathrm{d}z$ with

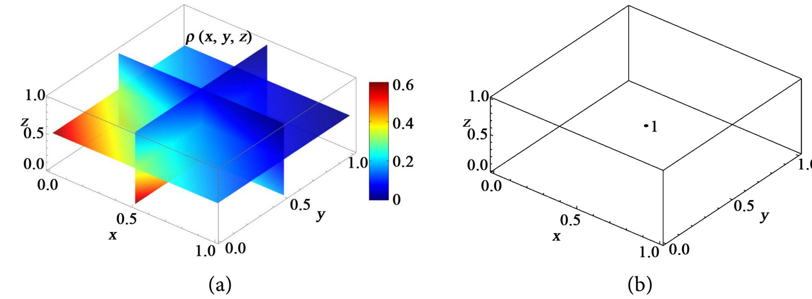

Figure 5. Spatial distribution of the volume density $\rho(x,y,z)$ (a) and concentrated density functions (b) relevant to the numerical Example 3.

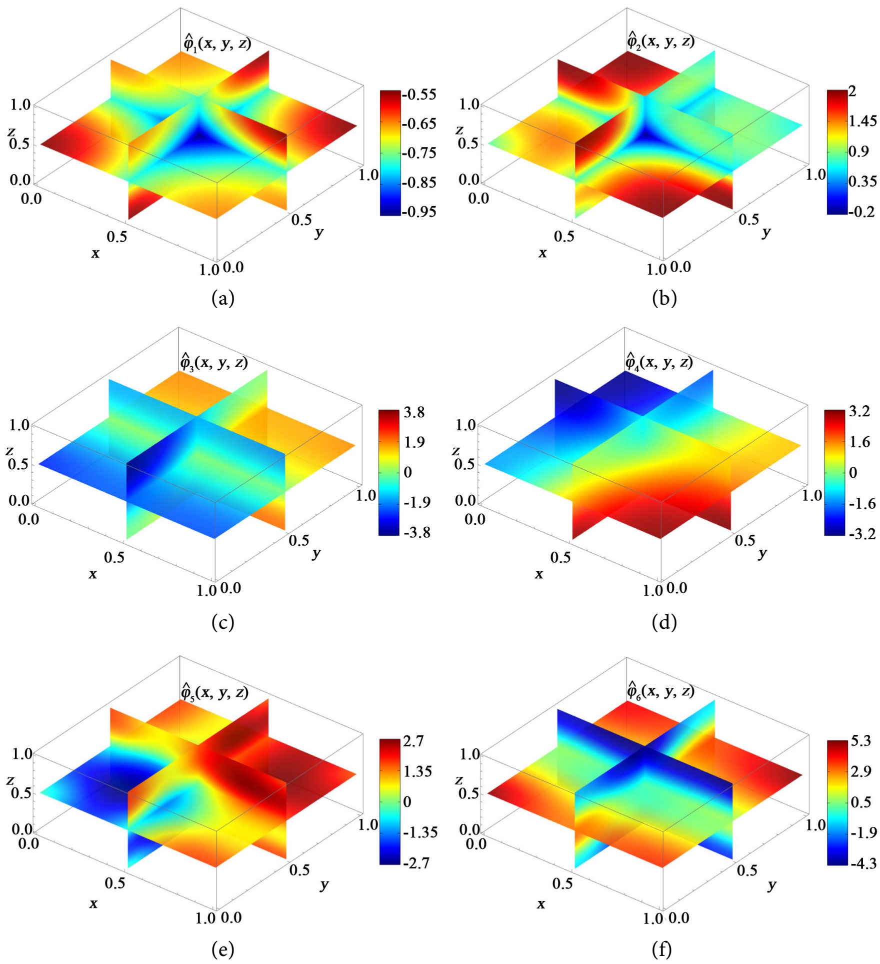

Figure 6. Spatial distribution of the approximate eigenfunctions $\hat{\varphi}_h(x,y,z)$ $(h=1,2,\cdots,6)$ relevant to the numerical Example 3.

$$\rho(x,y,z)=1+\cos\left[\frac{\pi}{2}(1-2x-3y-4z)\right],\text{ and }\quad m_h=3x_h+2y_h+z_h,$$

$$x_1=x_2=x_5=x_6=y_1=y_3=y_5=y_7=z_1=z_2=z_3=z_4=\frac{1}{4},$$

$$x_3=x_4=x_7=x_8=y_2=y_4=y_6=y_8=z_5=z_6=z_7=z_8=\frac{3}{4}\quad\text{for}\quad h=1,2,\cdots,8=H$$

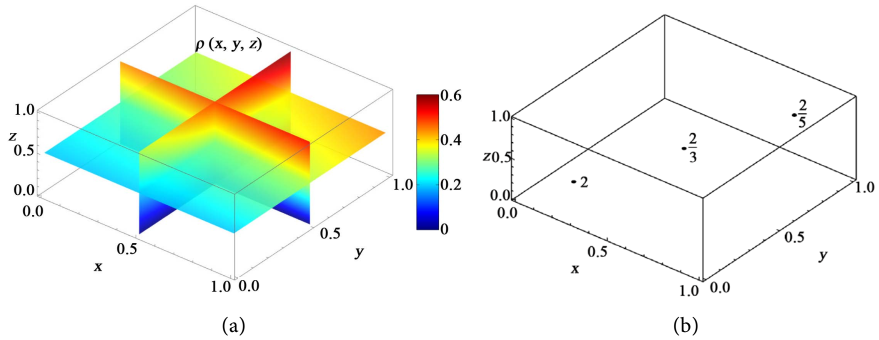

Figure 7. Spatial distribution of the volume density $\rho(x,y,z)$ (a) and concentrated density functions (b) relevant to the numerical Example 4.

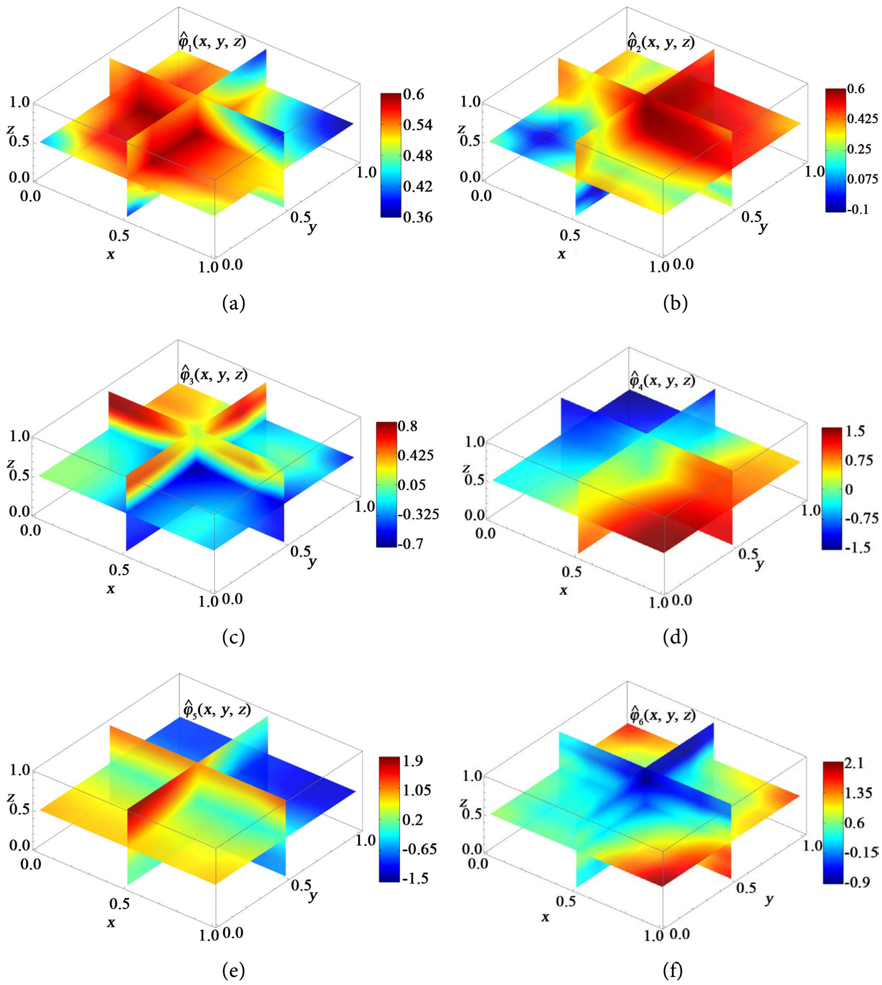

Figure 8. Spatial distribution of the approximate eigenfunctions $\hat{\varphi}_h(x,y,z)$ ($h = 1,2,\cdots,6$) relevant to the numerical Example 4.

(see **Figure 9**). Under this assumption, the approximate eigenvalues evaluated by using the Rayleigh-Ritz and inverse iteration methods are listed in **Table 5**, whereas the relevant eigenfunctions are shown in **Figure 10**.

Numerical Example 6

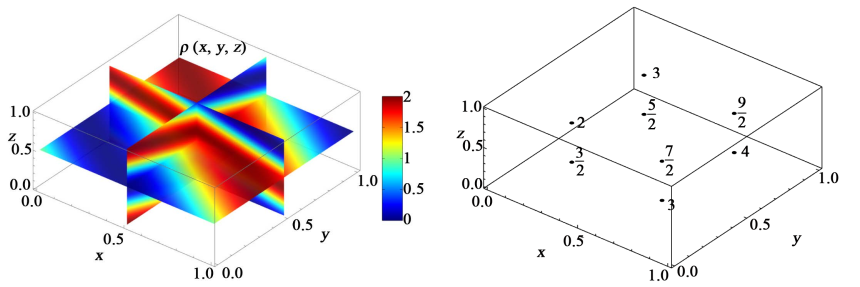

(a) (b)

Figure 9. Spatial distribution of the volume density $\rho(x,y,z)$ (a) and concentrated density functions (b) relevant to the numerical Example 5.

Table 3. Approximate eigenvalues $\tilde{\mu}_h$ and $\hat{\mu}_h$ ($h=1,2,\cdots,6$) relevant to the numerical Example 3, as computed by means of the Rayleigh-Ritz and inverse iteration method, respectively.

h	$\tilde{\mu}_h$	$\hat{\mu}_h$
1	0.827191	0.827079
2	0.0286952	0.0287715
3	0.0258541	0.0258874
4	0.0258541	0.0258874
5	0.0071926	0.00721217
6	0.00628217	0.00631337

Table 4. Approximate eigenvalues $\tilde{\mu}_h$ and $\hat{\mu}_h$ ($h=1,2,\cdots,6$) relevant to the numerical Example 2, as computed by means of the Rayleigh-Ritz and inverse iteration method, respectively.

h	$\tilde{\mu}_h$	$\hat{\mu}_h$
1	1.37202	1.38514
2	0.461313	0.439849
3	0.150812	0.148043
4	0.122611	0.121926
5	0.115747	0.115269
6	0.0456381	0.0440725

Table 5. Approximate eigenvalues $\tilde{\mu}_h$ and $\hat{\mu}_h$ ($h=1,2,\cdots,6$) relevant to the numerical Example 5, as computed by means of the Rayleigh-Ritz and inverse iteration method, respectively.

h	$\tilde{\mu}_h$	$\hat{\mu}_h$
1	11.6841	12.0167
2	3.25662	3.10980
3	3.18704	3.04593
4	1.27341	1.30780
5	0.211891	0.195245
6	0.147751	0.125519

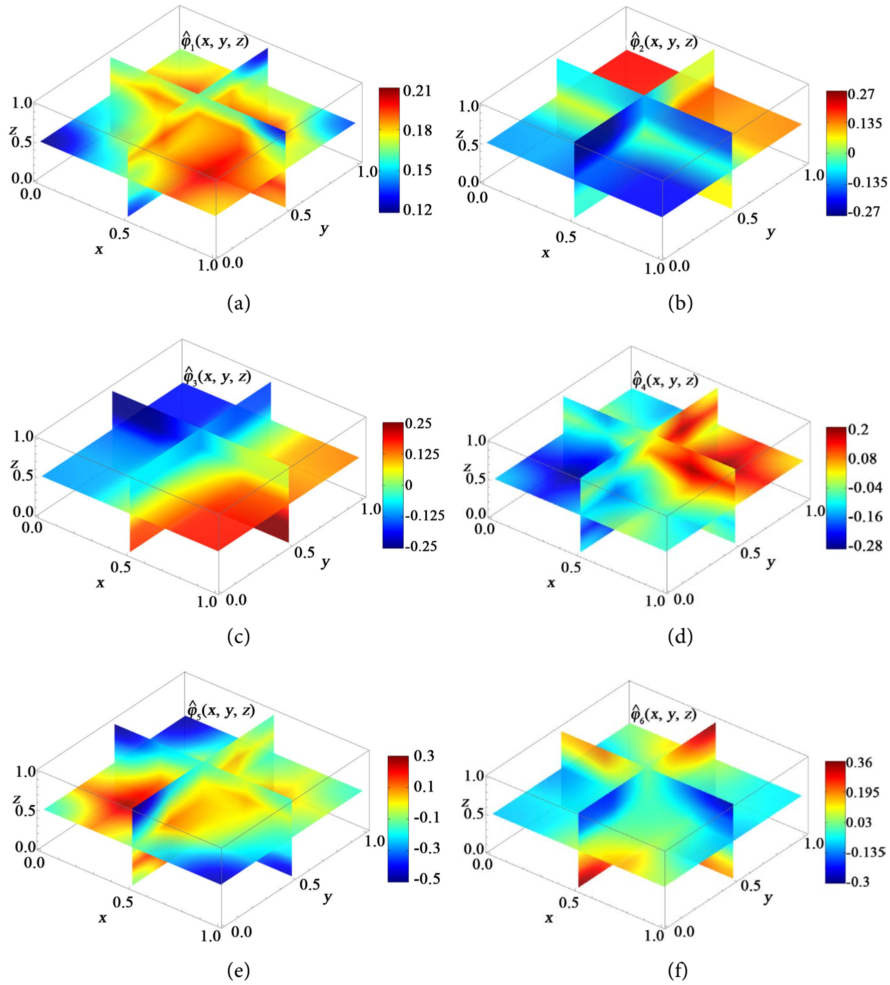

Figure 10. Spatial distribution of the approximate eigenfunctions $\hat{\varphi}_h(x, y, z)$ ($h = 1, 2, \cdots, 6$) relevant to the numerical Example 5.

Let $a = b = c = 1$, and

$$\begin{aligned} dM &= \rho(x, y, z)\,dxdydz + \sigma(x, y, z)\,\delta(z - \zeta_s)\,dxdydz \\ &+ \sum\nolimits_h \delta(x - x_h)\,\delta(y - y_h)\,\delta(z - z_h)\,dxdydz \end{aligned}$$

with $\rho(x, y, z) = \left[\cosh(2y - x) + \sin(2x - y)\right] / \left(1 + e^{x+y}\right)$, $\sigma(x, y, z) = e^{-2x-3y+4z}$, $\zeta_s = \frac{1}{4}$, and $x_h = 1 - y_h = \frac{1}{H}\left(h - \frac{1}{2}\right)$, $z_h = \frac{4}{5}$ for $h = 1, 2 = H$ (see **Figure 11**). Under this assumption, the approximate eigenvalues evaluated by using the Rayleigh-Ritz and inverse iteration methods are listed in **Table 6**, whereas the relevant eigenfunctions are shown in **Figure 12**.

Numerical Example 7

Let $a = b = c = 1$, and

$$\begin{aligned} dM &= \rho(x, y, z)\,dxdydz + \sigma(x, y, z)\,\delta(x - \xi_s)\,dxdydz \\ &+ \sum\nolimits_h m_h \delta(x - x_h)\,\delta(y - y_h)\,\delta(z - z_h)\,dxdydz \end{aligned}$$

with $\rho(x, y, z) = \operatorname{sech}\left(4\left[(x - 1/2)^2 + (y - 1/2)^2 + (z - 1/2)^2\right]^{1/2}\right)$,

$\sigma(x, y, z) = 5x + \sin(2y)\cos(3z)$, $\xi_s = \frac{1}{5}$, and $m_h = y_h + z_h$, $x_h = \frac{3}{4}$,

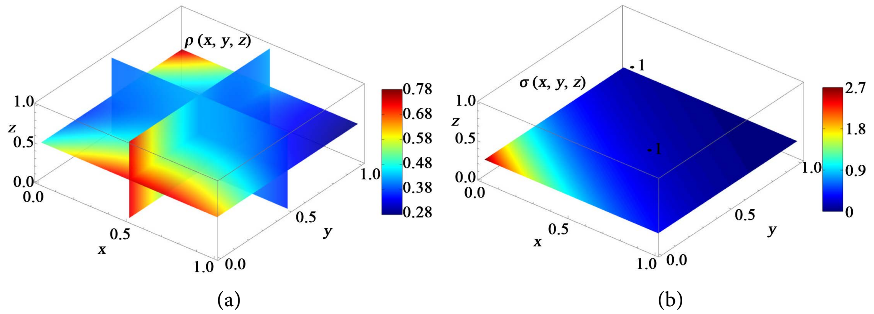

Figure 11. Spatial distribution of the volume density $\rho(x,y,z)$ (a) and concentrated density functions (b) relevant to the numerical Example 6.

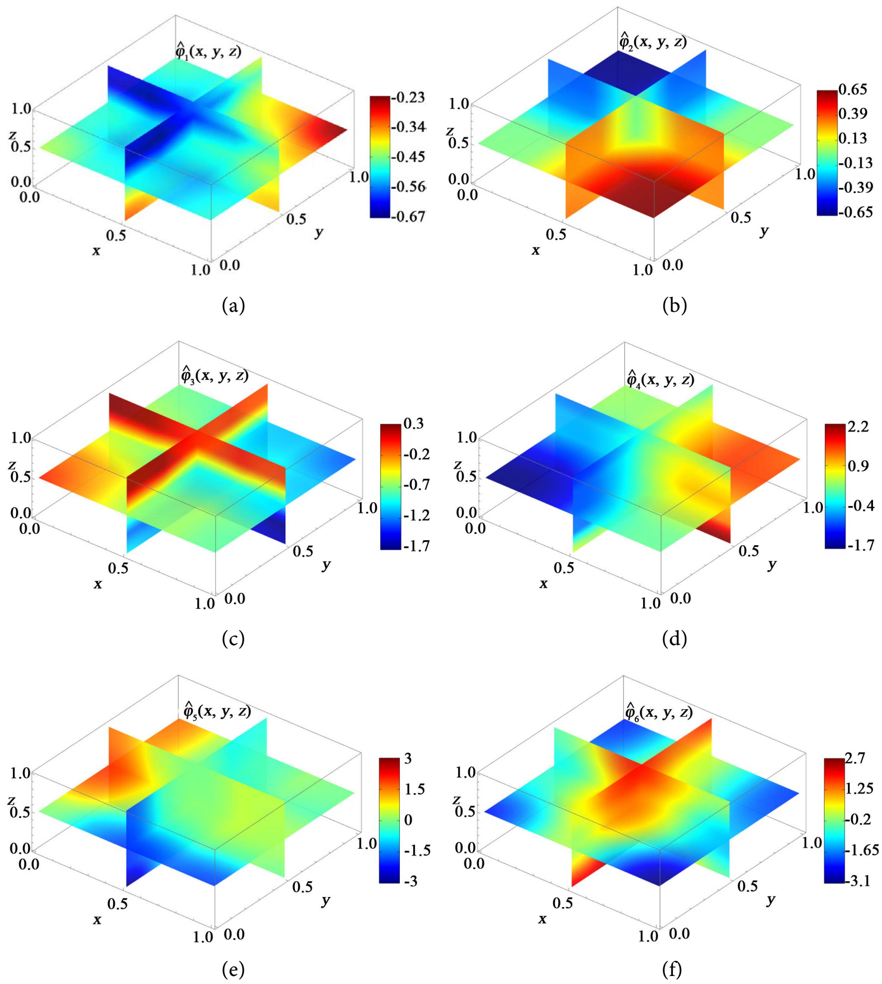

Figure 12. Spatial distribution of the approximate eigenfunctions $\hat{\varphi}_h(x,y,z)$ ($h=1,2,\cdots,6$) relevant to the numerical Example 6.

$y_h = z_h = \frac{1}{H}\left(h-\frac{1}{2}\right)$ for $h=1,2,3=H$ (see **Figure 13**). Under this assumption, the approximate eigenvalues evaluated by using the Rayleigh-Ritz and inverse iteration methods are listed in **Table 7**, whereas the relevant eigenfunctions are shown in **Figure 14**.

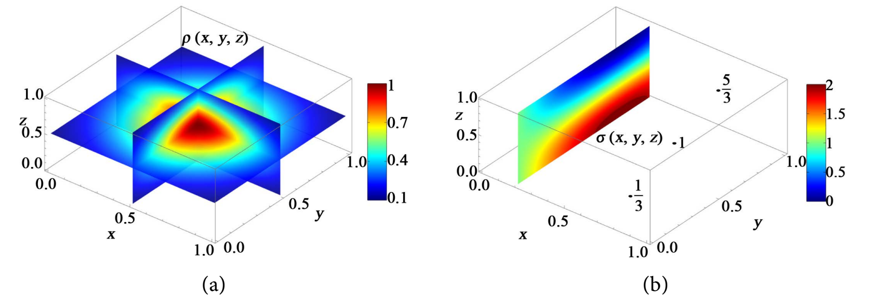

Figure 13. Spatial distribution of the volume density $\rho(x, y, z)$ (a) and concentrated density functions (b) relevant to the numerical Example 7.

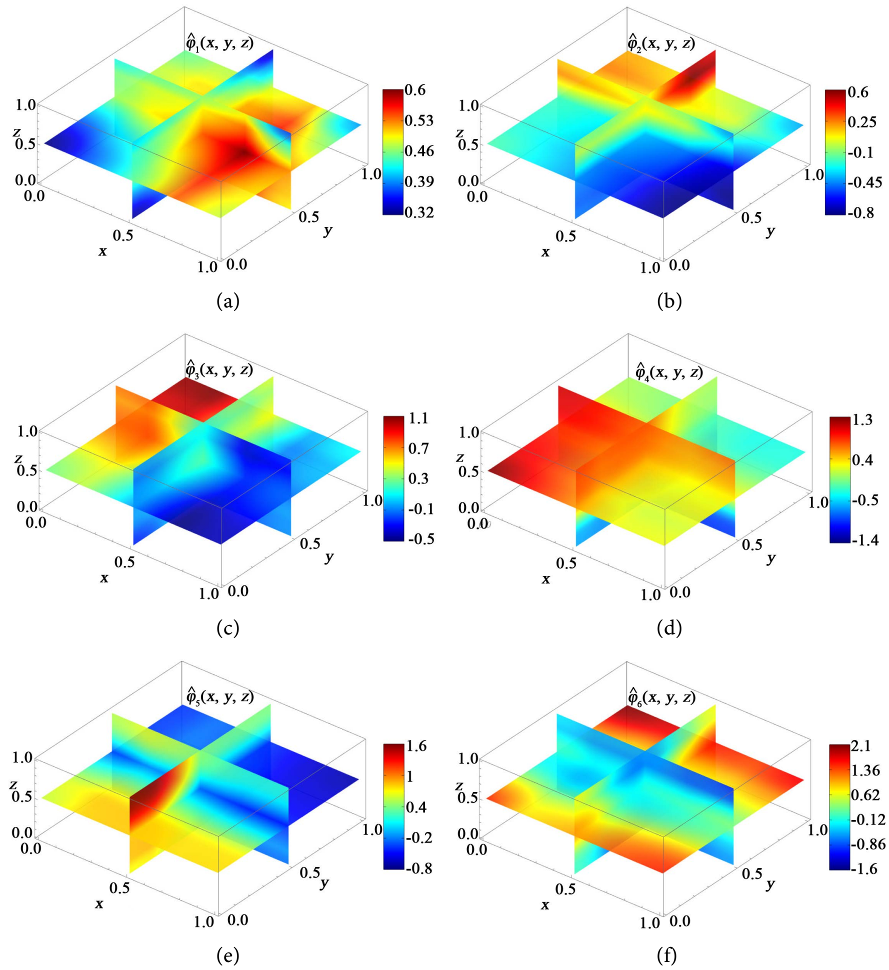

Figure 14. Spatial distribution of the approximate eigenfunctions $\hat{\varphi}_h(x, y, z)$ ($h = 1, 2, \cdots, 6$) relevant to the numerical Example 7.

Numerical Example 8

Let $a = b = c = 1$, and

$$\mathrm{d}M = \rho(x, y, z)\mathrm{d}x\mathrm{d}y\mathrm{d}z + \sigma(x, y)\delta(z - \zeta_s(x, y))\mathrm{d}x\mathrm{d}y\mathrm{d}z + \delta\left(x - \frac{3}{4}\right)\delta\left(y - \frac{3}{4}\right)\delta\left(z - \frac{3}{4}\right)\mathrm{d}x\mathrm{d}y\mathrm{d}z$$

Table 6. Approximate eigenvalues $\tilde{\mu}_h$ and $\hat{\mu}_h$ ($h = 1, 2, \cdots, 6$) relevant to the numerical Example 6, as computed by means of the Rayleigh-Ritz and inverse iteration method, respectively.

h	$\tilde{\mu}_h$	$\hat{\mu}_h$
1	1.46677	1.48646
2	0.636561	0.607952
3	0.142093	0.142025
4	0.0434152	0.0451649
5	0.0287695	0.0298745
6	0.0179072	0.0179560

Table 7. Approximate eigenvalues $\tilde{\mu}_h$ and $\hat{\mu}_h$ ($h = 1, 2, \cdots, 6$) relevant to the numerical Example 7, as computed by means of the Rayleigh-Ritz and inverse iteration method, respectively.

h	$\tilde{\mu}_h$	$\hat{\mu}_h$
1	1.71928	1.75065
2	0.404514	0.391333
3	0.327108	0.328006
4	0.155119	0.152451
5	0.133601	0.132340
6	0.0390550	0.0389560

with $\rho(x,y,z) = [3 + 2\cos(xz) + \sin(yz)]/(1 + 2x + 3y + 4z)$, and $\sigma(x,y) = (1 + 2x + 3y)/[7 + \cos(6y) + \sin(5x)]$, $\zeta_s(x,y) = \frac{1}{2}[1 + \cos(x) - \sin(3y)]$ (see **Figure 15**). Under this assumption, the approximate eigenvalues evaluated by using the Rayleigh-Ritz and inverse iteration methods are listed in **Table 8**, whereas the relevant eigenfunctions are shown in **Figure 16**.

Numerical Example 9

Let $a = b = c = 1$, and

$$\begin{aligned} \mathrm{d}M = {} & \rho(x,y,z)\,\mathrm{d}x\mathrm{d}y\mathrm{d}z + \sigma(x,y)\,\delta(z - \zeta_s(x,y))\,\mathrm{d}x\mathrm{d}y\mathrm{d}z \\ & + \tau(z)\,\delta(x - \xi_l(z))\,\delta(y - \eta_l(z))\,\mathrm{d}x\mathrm{d}y\mathrm{d}z \\ & + \sum\nolimits_h m_h \delta(x - x_h)\,\delta(y - y_h)\,\delta(z - z_h)\,\mathrm{d}x\mathrm{d}y\mathrm{d}z \end{aligned}$$

with $\rho(x,y,z) = 4 + 3\cos(3x) + 2\sin(2y) + \tan(z)$, $\sigma(x,y) = 2\log(1 + y + xy)$, $\zeta_s(x,y) = \frac{1}{4}(1 - x + 2y)$, $\tau(z) = 2z$, $\xi_l(z) = \eta_l(z) = 4z - 3$, and $m_h = x_h + y_h + z_h$, $x_1 = x_2 = y_1 = y_3 = \frac{1}{4}$, $x_3 = x_4 = y_2 = y_4 = \frac{3}{4}$, $z_h = \frac{2}{3}$ for

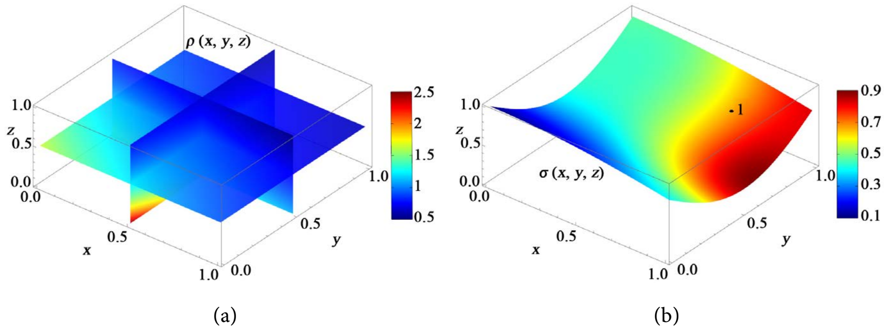

Figure 15. Spatial distribution of the volume density $\rho(x, y, z)$ (a) and concentrated density functions (b) relevant to the numerical Example 8.

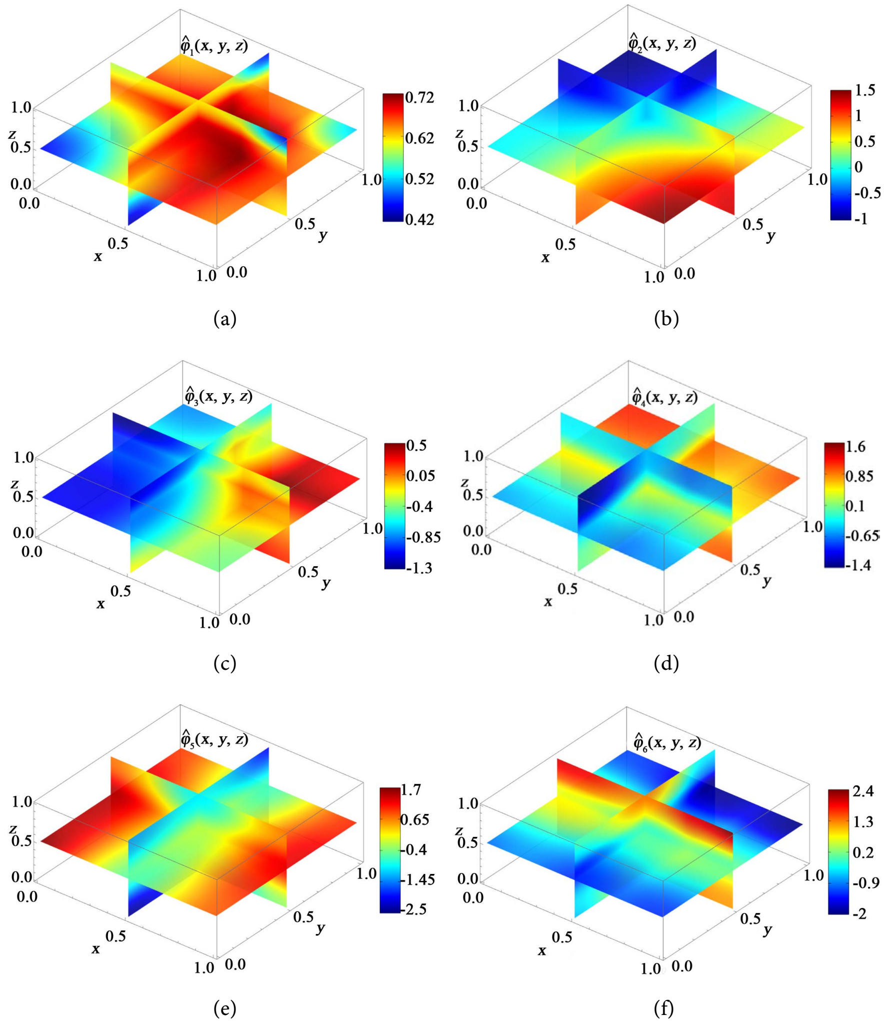

Figure 16. Spatial distribution of the approximate eigenfunctions $\hat{\varphi}_h(x, y, z)$ ($h = 1, 2, \cdots, 6$) relevant to the numerical Example 8.

$h = 1, 2, 3, 4 = H$ (see **Figure 17**). Under this assumption, the approximate eigenvalues are evaluated as in **Table 9**, whereas the relevant eigenfunctions are shown in **Figure 18**.

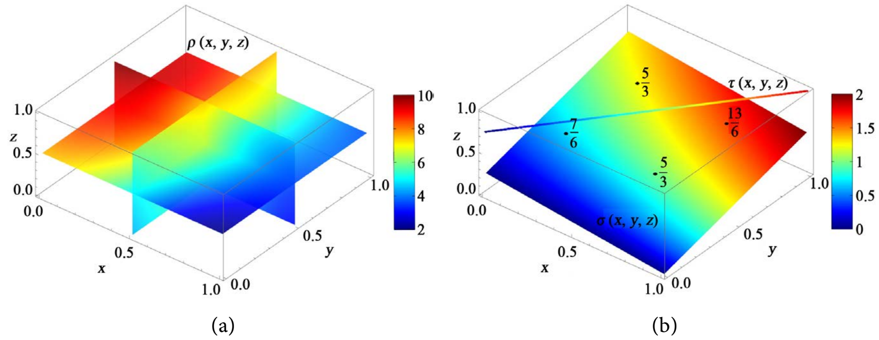

Figure 17. Spatial distribution of the volume density $\rho(x,y,z)$ (a) and concentrated density functions (b) relevant to the numerical Example 9.

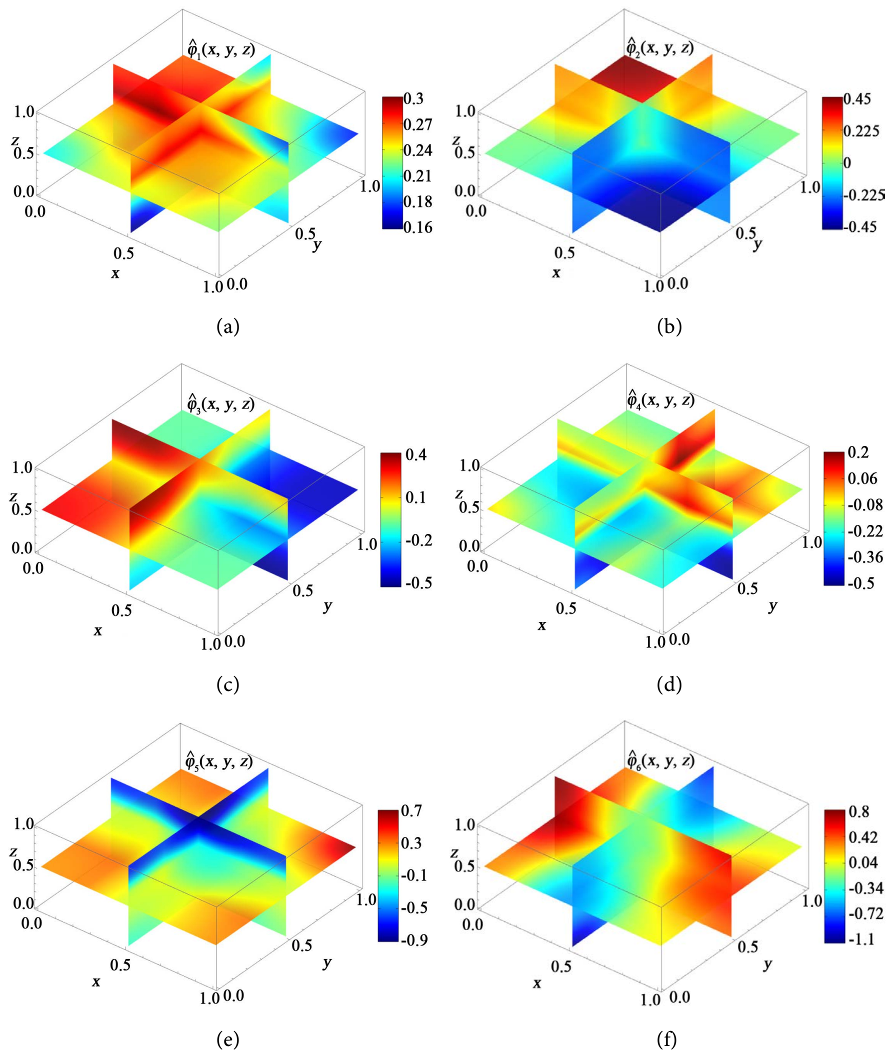

Figure 18. Spatial distribution of the approximate eigenfunctions $\hat{\varphi}_h(x,y,z)$ ($h = 1, 2, \cdots, 6$) relevant to the numerical Example 9.

Acknowledgements

This study has been partly carried out in the framework of the research and

Table 8. Approximate eigenvalues $\tilde{\mu}_h$ and $\hat{\mu}_h$ ($h = 1, 2, \cdots, 6$) relevant to the numerical Example 8, as computed by means of the Rayleigh-Ritz and inverse iteration method, respectively.

h	$\tilde{\mu}_h$	$\hat{\mu}_h$
1	1.24996	1.28312
2	0.232580	0.236340
3	0.212298	0.213581
4	0.175619	0.177549
5	0.0535925	0.0541850
6	0.0451690	0.0465835

Table 9. Approximate eigenvalues $\tilde{\mu}_h$ and $\hat{\mu}_h$ ($h = 1, 2, \cdots, 6$) relevant to the numerical Example 9, as computed by means of the Rayleigh-Ritz and inverse iteration method, respectively.

h	$\tilde{\mu}_h$	$\hat{\mu}_h$
1	6.85505	6.97836
2	1.56685	1.51732
3	1.18747	1.16698
4	0.588232	0.594839
5	0.301015	0.320349
6	0.197606	0.200069

development program running at *The Antenna Company*, and is funded by the Competitiveness Enhancement Program grant at Tomsk Polytechnic University.

References

[1] Mikhlin, S.G. (1964) Integral Equations and Their Applications. 2nd Edition, Pergamon Press, Oxford.

[2] Zaanen, A.C. (1953) Linear Analysis. Measure and Integral, Banach and Hilbert Space, Linear Integral Equations. Interscience Publ. Inc., New York, North Holland Publ. Co., Amsterdam, P. Noordhoff N.V., Groningen.

[3] Anselone, P.M. (1971) Collectively Compact Operator Approximation Theory and Application to Integral Equations. Prentice-Hall Series in Automatic Computation. Prentice-Hall, Inc., Englewood Cliffs.

[4] Miranda, C. (1992) Opere Scelte. Cremonese, Roma.

[5] Miranda, C. (1938) Alcune generalizzazioni delle serie di funzioni ortogonali e loro applicazioni. [On Some Generalizations of Orthogonal Function Series Expansions and Relevant Applications.] *Rend. Sem. Mat. Torino*, **7**, 5-17.

[6] Jung, I.H., Kwon, K.H., Lee, D.W. and Littlejohn, L.L. (1995) Sobolev Orthogonal Polynomials and Spectral Differential Equations. *Transactions of the American Mathematical Society*, **347**, 3629-3643.
https://doi.org/10.1090/S0002-9947-1995-1308015-9

[7] Marcellán, F., Pérez, T.E., Piñar, M.A. and Ronveaux, A. (1996) General Sobolev Orthogonal Polynomials. *Journal of Mathematical Analysis and Applications*, **200**, 614-634. https://doi.org/10.1006/jmaa.1996.0227

[8] Natalini, P. and Ricci, P.E. (2006) Computation of the Eigenvalues of Fredholm-Stieltjes Integral Equations. *Applicable Analysis*, **85**, 607-622. https://doi.org/10.1080/00036810500397039

[9] Natalini, P., Patrizi, R. and Ricci, P.E. (2006) Eigenfunctions of a Class of Fredholm-Stieltjes Integral Equations via the Inverse Iteration Method. *Journal of Applied Functional Analysis*, **1**, 165-181.

[10] Caratelli, D., Natalini, P. and Ricci, P.E. (2017) Computation of the Eigenvalues of 2D "Charged" Integral Equations.

[11] Fichera, G. (1973) Abstract and Numerical Aspects of Eigenvalue Theory. Lecture Notes, The University of Alberta, Dept. of Math., Edmonton.

[12] Fichera, G. (1978) Numerical and Quantitative Analysis. Surveys and Reference Works in Mathematics, Pitman, Boston, London.

[13] Natalini, P., Noschese, S. and Ricci, P.E. (1999) An Iterative Method for Computing the Eigenvalues of Second Kind Fredholm Operators and Applications. *Leganés*, **9**, 128-136.

[14] Widder, D.V. (1999) Advanced Calculus. 3rd Edition, Dover Publ. Inc., New York.